Structural and Electronic properties of Layered Arsenic and Antimony Arsenide

Liangzhi Kou[1*], Yandong Ma[2], Xin Tan[1], Thomas Frauenheim[3], Aijun Du[4], and Sean Smith[1*]

[1.] Integrated Materials Design Centre (IMDC), School of Chemical Engineering, University of New South Wales, Sydney, NSW 2052, Australia

[2.] School of Engineering and Science, Jacobs University Bremen, Campus Ring 1, 28759 Bremen, Germany

[3.] Bremen Center for Computational Materials Science, University of Bremen, Am Falturm 1, 28359 Bremen, Germany

[4.] School of Chemistry, Physics and Mechanical Engineering, Queensland University of Technology, Brisbane, QLD 4001, Australia

E-mail: kouliangzhi@gmail.com; sean.smith@unsw.edu.au

Abstract

Layered materials exhibit intriguing electronic characteristics and the search for new types of two-dimensional (2D) structures is of importance for future device fabrication. Using state-of-art first principle calculations, we identify and characterize the structural and electronic properties of two 2D layered arsenic materials, namely arsenic and its alloy AsSb. The stable 2D structural configuration of Arsenic is confirmed to be the low buckled two-dimensional hexagonal structure by phonon and binding energy calculations. The monolayer exhibits the indirect semiconducting properties with gap around 1.5 eV (corrected to 2.2 eV by hybrid function), which can be modulated into a direct semiconductor within a small amount of tensile strain. These semiconducting properties are preserved when cutting into 1D nanoribbons, but the indirect and direct gap depends on the edge. It is interesting to find that an indirect to direct gap transition can be achieved under strain modulation of the armchair ribbon. Essentially the same phenomena can be found in layered AsSb, except a weak Rashba induced band splitting is present in AsSb due to the non-symmetric structure and spin orbit coupling. When an additional layer is added on the top, a semiconductor-metal transition will occur. The findings here broaden the family of 2D materials beyond graphene and transition metal dichalcogenides and provide useful information for experimental fabrication of new layered materials with possible application in optoelectronics.

KEYWORDS: 2D materials, Arsenic, Electronic properties, Density functional theory

Introduction

Owing to their remarkable properties,[1,2] in recent years graphene-like 2D materials have attracted much research attention as emerging materials for nanoelectronics. As exemplified by recently synthesized graphene,[3,4] silicene,[5-7] boron-nitride nanosheets,[8-10] transition-metal dichalcogenides (TMDs),[11] and black phosphorous,[12,13] these materials are theoretically predicted and experimentally confirmed to possess novel properties which are different from or even better than their bulk counterparts. These 2D layered materials can exhibit versatile electronic properties, including metallic, semiconducting, superconducting, and even topological insulator[14] properties with extremely high mobility. With many promising applications in nanoelectronics and optoelectronics such as field-effect transistors (FETs), optoelectronics devices, photovoltaic solar cells, valley electronics and spintronics applications.[11,15,16] they are considered to represent a relatively new and exciting area for nanotechnology. In this context, both the fundamental scientific importance and the promise of practical applications makes the exploration of new layered materials with novel properties a vigorous field of research in condensed matter physics and materials research.

The 2D layered materials with single elemental constitution that have currently been synthesized/fabricated are mainly located right part of periodic table, namely groups IV and V. For example, the commonly studied graphene,[3] silicene, germanium[17] and tin films[18] with honeycomb lattices are composed with group IV elements. Phosphorene with a puckered honeycomb structure,[12,13] antimony and bilayer bismuth[19,20] in the buckled honeycomb configuration are group V elements. Excepting the gas nitrogen and arsenic, all the 2D layered structures associated with group IV and V elements have been experimentally fabricated and intriguing electronic properties have been predicted theoretically. Although there is no report of monolayer arsenic, bulk arsenic has been extensively studied. Three most common arsenic allotropes are metallic grey, yellow and black arsenic, with grey being the most common and stable form.[21] Grey arsenic (α-As, space group R3m) adopts a double-layered structure consisting of many interlocked rufied six-membered rings. Because of weak bonding between the layers, grey arsenic is brittle and has a relatively low Mohs hardness of 3.5. Nearest and next-nearest neighbours form a distorted octahedral complex, with the three atoms in the same double-layer being slightly closer than the three atoms in the next. Due to the weak bonding between layers, it is possible to fabricate the monolayer using a micromechanical cleavage method like graphene. However, the detailed atomic structure

(buckled, planar or a puckered-like structure), electronic properties (metallic or semiconducting) and possible electronics applications are not clear yet. The answers to these questions will be important for the potential utility of layered arsenic in future devices.

In this Letter, we have studied the structural characteristics and corresponding electronic properties of layered arsenic and its alloy AsSb using first principle calculations. Unlike the puckered honeycomb structure of phosphorene within the same family, monolayer arsenic exhibits a low-buckled two-dimensional hexagonal structure. Since the interlayer interaction is dominated by the weak van der Waals force, monolayer arsenic is suggested to be experimentally obtainable based on micromechanical cleavage and exfoliation methods from bulk grey arsenic.[21] Under equilibrium conditions, monolayer arsenic is an indirect semiconductor with a predicted band gap of 1.5 eV (2.2 eV from hybrid functional calculations). With a hydrostatic biaxial strain, one can observe an indirect-direct band transition (2%) while the gap is further reduced with increased strain deformation. When an additional arsenic layer is added on the top (bilayer arsenic), the system becomes metallic. For the case of the corresponding 1D nanoribbons, edge-shape dependent indirect-direct band behaviour is found, which is also thunable with applied strain. The alloy AsSb has similar structural and electronic features except for an obvious band splitting due to the Rashba effect arising from the asymmetric structure.

Methods

First-principle calculations based on density functional theory (DFT) were carried out using the Vienna Ab Initio Simulation Package (VASP).[22] The exchange correlation interaction was treated within the generalized gradient approximations (GGA)[23] of Perdew-Burke-Ernzerhof (PBE). Both the materials are periodic in the xy plane and separated by at least 10 Å along the z direction to avoid the interactions between adjacent models. To correct the well-known underestimation of band gap in LDA or PBE calculation, the hybrid functional methods, hybrid Heyd-Scuseria-Ernzerhof (HSE),[24] are introduced, which has been proven to get the band gap value close to experiments. All the atoms in the unit cell are fully relaxed until the force on each atom is less than 0.01 eV/Å. The Brillouin-zone integration was sampled by a 14×14×1 k-grid mesh. An energy cutoff of 400 eV was chosen for the plane wave basis. To describe the vdW interaction, a semi-empirical correction by Grimme method was adopted.[25] Spin orbit coupling effects are also included in electronic calculations. We use the CASTEP

code[26] to calculate the phonon dispersion relations and the finite displacement method and PBE are employed.

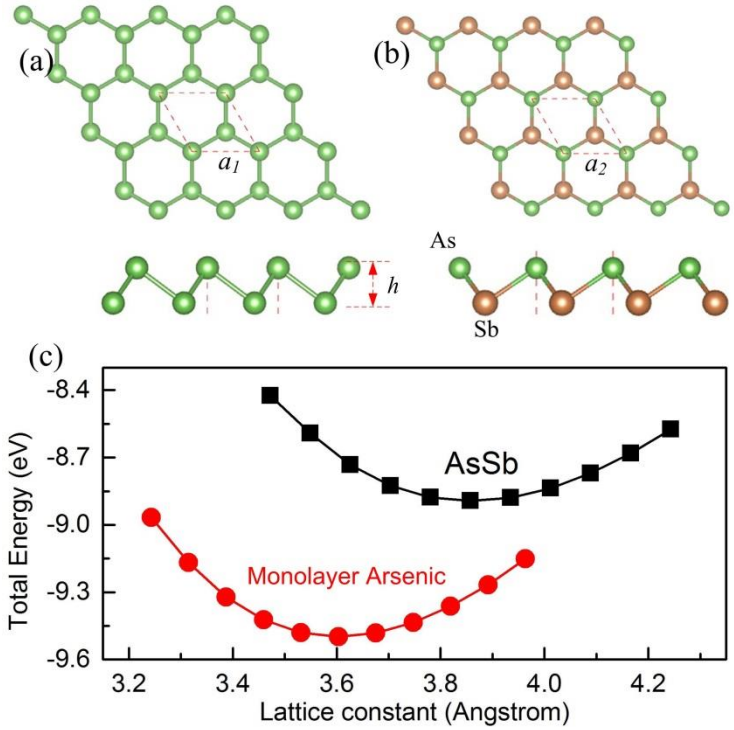

Figure 1: (color online) (a) Top and side view of monolayer arsenic. The studied unit cell is indicated with dashed rhombus. Lattice constant is labelled with a_1 while the height due to buckled configurations is marked with h. The corresponding model of AsSb is presented in (b). Total energies as a function of lattice constants are displayed in (c).

Results and discussion

Before the detailed electronic investigations, we firstly determine the structural characteristics of monolayer arsenic. As neighbours of arsenic at group V in the periodic table, black phosphorous exhibits the puckered honeycomb structure while antimony is in the buckled honeycomb configuration. Two similar models for monolayer arsenic (one like phosphorous and another like antimony) are therefore constructed to examine which one is more stable. From the structural relaxing calculations, it is found that the puckered honeycomb structure eventually evolves into the layered buckled shape, which indicates that the configuration analogous to black phosphorous is not stable. However, the low-buckled hexagonal structure keeps its original shape as shown in Fig. 1a, suggesting that it could exist in reality. Actually the obtained buckled structure corresponds to the layer in bulk grey

arsenic (α-As, which is the most common arsenic allotrope).[21] In the following part, our investigations will focus on this configuration.

The structure of monolayer arsenic is shown in Fig. 1. We obtained the stable low-buckled geometry of minimum energy with lattice constant a_1=3.6 Å (see Fig. 1c) and nearest neighbour As-As distance d=2.51 Å through structural optimization. Compared with graphene, the larger As-As interatomic distance weakens the π-π overlaps, so it cannot maintain the planar structure anymore. This results in a low-buckled structure with sp^3-like hybrid orbitals. In Fig. 1(a), one can define the buckling height along z direction, h, which is 1.4 Å from the structural relaxation.

To further demonstrate its stability, we calculated the binding energy, which is defined as $E_b=E_{tot}/n-E_{As}$, where E_{tot} is the total energy of 2D arsenic layer while E_{As} is the energy of single As atom and n is the number of As. The E_b is calculated to be -2.96 eV/atom, which is comparable with the corresponding graphene value. We further confirmed the dynamic stability of the thin film by calculating their phonon spectra, and the corresponding result is displayed in Figure 2. All phonon branches are positive, confirming the dynamic stability.

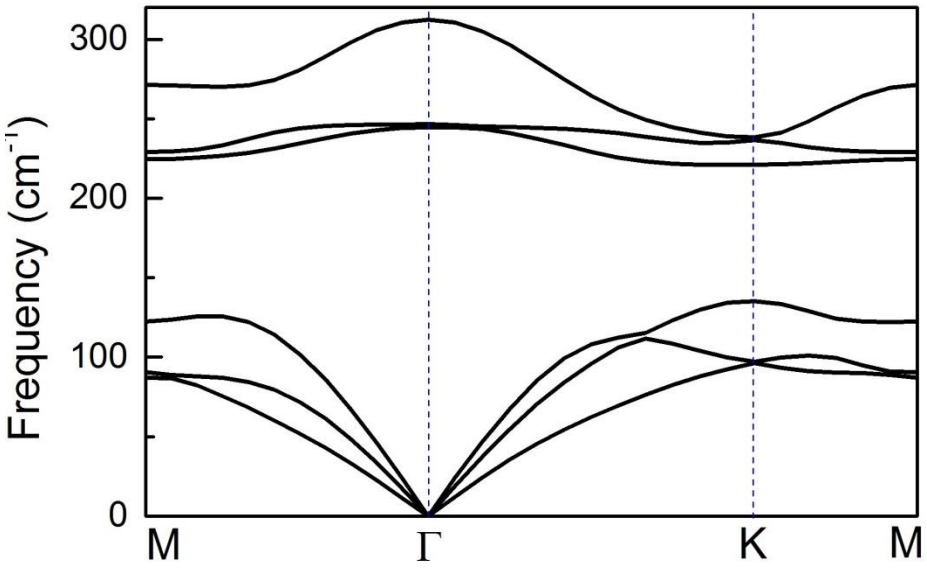

Figure 2: Phonon frequency of 2D arsenic layer.

With the optimized structures of monolayer arsenic and confirmed structural stability, we now turn our attentions to the electronic properties. The calculated band structures are shown in Figure 3. Our calculations clearly show that monolayer arsenic is an indirect

semiconductor although the corresponding bulk structure exhibits metallic properties. For monolayer arsenic, the valence band maximum (VBM) is located at Γ point, but the conduction band minimum (CBM) is at the half way along M to Γ, see Fig. 2(a). The indirect band gap of monolayer arsenic is 1.52 eV (as indicated by the dashed red arrow), which is slightly smaller than the gap value of 1.94 eV at Γ point. From the orbital decomposition in Fig. 3(c), we can see that the CBM state at Γ point comprises mainly of the p_z orbit of As while the global CBM located at half-way between M-Γ comprises mainly of p_y, which means that the external deformation will have different effects on the two states and lead to indirect-direct transition, as revealed in the following. Due to the presence of artificial self-interaction and the absence of the derivative discontinuity in the exchange-correlation potential, DFT in the LDA and GGA, suffers from the underestimation of the band gap compared with their experimental values. In order to correct the GGA/LDA band-gaps, we used HSE functional. In the HSE approach, the exchange potential is separated into a long range and a short- range part. The 1/4 of the PBE exchange is replaced by the Hartree-Fock (HF) exact exchange and the full PBE correlation energy is added. HSE is shown to correct the GGA band gaps significantly by partially correcting the self-interaction. From the calculated bandstructure (black lines in Figure 3a), the sharps of band states from PBE and HSE are basically the same, the indirect band gap is still predicted within the hybrid functional calculations, but the gap value is increased to 2.2 eV.

For optoelectronic applications, the semiconductors with direct band gap of 1-2 eV, like GaAs or InAs,[27,28] are desirable. Although the band gap of our studied monolayer arsenic is within the desirable range, one disadvantage is that the gap is indirect. In order to solve the problem and investigate the effect of external field on electronic properties, we checked the gap variation of the layered materials under hydrostatic biaxial tensile strain as shown in Fig. 3d. We have shown that the material will undergo an indirect to direct band transition under small tensile strain deformation. After the critical strain of 2%, monolayer arsenic becomes a direct band gap semiconductor at the Γ point as shown from the band state variations under strain deformation.

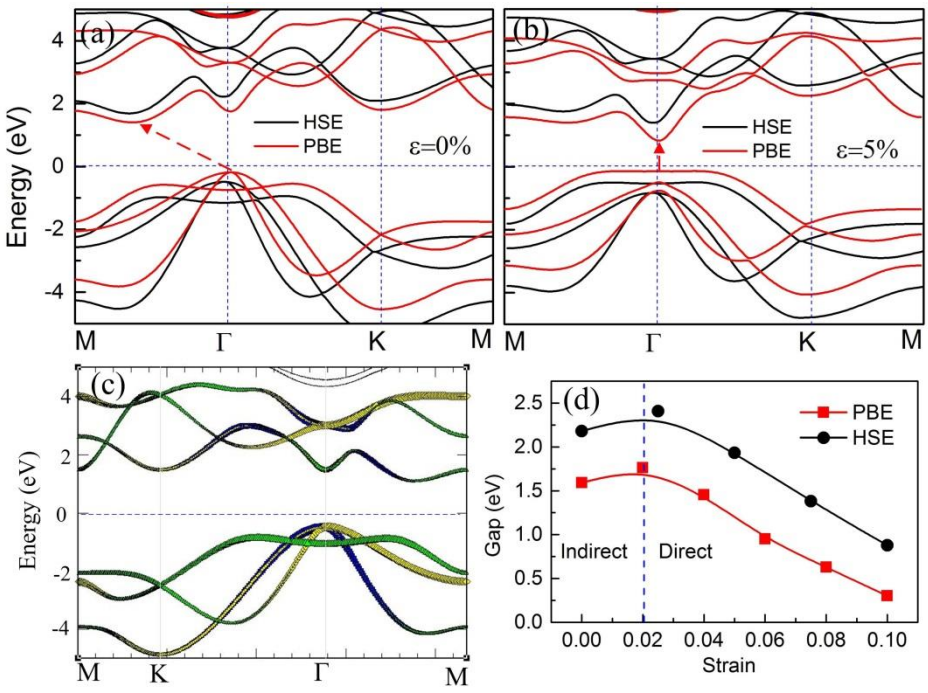

Figure 3: (colour online) (a) Bandstructures of monolayer arsenic under strain-free state, the red lines are for PBE calculations while the black ones are from HSE calculations. (b) The corresponding electronic structures under strain of 5%. (c) The orbit decomposition of bandstructure, red is s orbit, while blue, yellow and green are p_x, p_y and p_z, respectively. (d) Band gap variation under strain.

We show one representative example of the band structure under strain of 5% in Fig. 3b. The CBM state at the Γ point is sensitive to strain, which is significantly shifted downwards. In contrast, the original CBM located half-way between M-Γ (Fig. 3a) is moved significantly upwards under strain due to the different response of p_y and p_z orbitals to the strain deformation. The shifting of these band states leads to the reduction of band gap as well as the indirect-to-direct gap transition. The band gaps will be further reduced linearly under increased strain deformation, and it is about 0.2 eV when the strain reaches up to 10%. Both the PBE and HSE calculations predict the same trend except the underestimation from general DFT calculation, indicating the validity of the results and that PBE is capable of predicting the right trend. The effect of larger strain deformation is not investigated here since it is hard to be achieved experimentally and would likely cause possible structural damage. It is noted that monolayer arsenic keeps the low-buckled hexagonal shape even at a strain of 10% and does not become planar like graphene. By checking the height along the z direction, the values for both systems are reduced lineally, but the buckling heights are still larger than 1.3 Å even under strain of 10%.

When one additional arsenic layer is added on top to create bilayer arsenic, one can observe a significant change of electronic properties (not shown here). The conduction bands are significantly shifted downwards to the Fermi level, while valence bands are also moved upwards. As a result, the VBM of bilayer arsenic is not located at Γ anymore, but forms a "M" shaped state, leading to a semimetal with a pseudogap like the bulk case (α-As, semi metallic). We attribute the underlying mechanism to relatively strong interlayer interactions; the distance between layers is 2.32 Å, which is within van der Waals interaction range, but without chemical bonding between layers.

Due to quantum confinement effects and the edge states, 1D derivative materials always display some exotic properties that differ from the parent 2-D materials. For example, graphene nanoribbons with small width are semiconductors while 2D graphene is metallic. To check possible new features and give a comprehensive picture of layered arsenic materials, we cut the 2D monolayer arsenic into ribbons. According to the edges, two types of ribbons are obtained, armchair and zigzag. All the edge atoms are passivated with hydrogen to remove the dangling bands. It is interesting to find that the indirect band gap is inherited by the armchair nanoribbons, but not zigzag one. All armchair ribbons possess indirect gap, the value of which decreases with increasing width and approaches to the bulk one as shown in Fig. 4. For example, the gap of armchair ribbon with width of 2 nm is large as 2 eV due to the confinement effect, but reduced to 1.7 eV when the width increases to 3.6 nm. In contrast, all zigzag ribbons exhibit direct gaps at the Γ point. Similar to the bulk arsenic layer, the strain along periodic direction can also modulate the band gap value and induce indirect-direct gap transition. As shown Fig. 4a, the indirect gap of an armchair ribbon can be turned into a direct one when 7.5% strain is applied, while the gap value is reduced from 1.65 eV to 1.5 eV. However, the strain along zigzag direction only reduces the band gap as shown in Fig. 4(b) and 4(d).

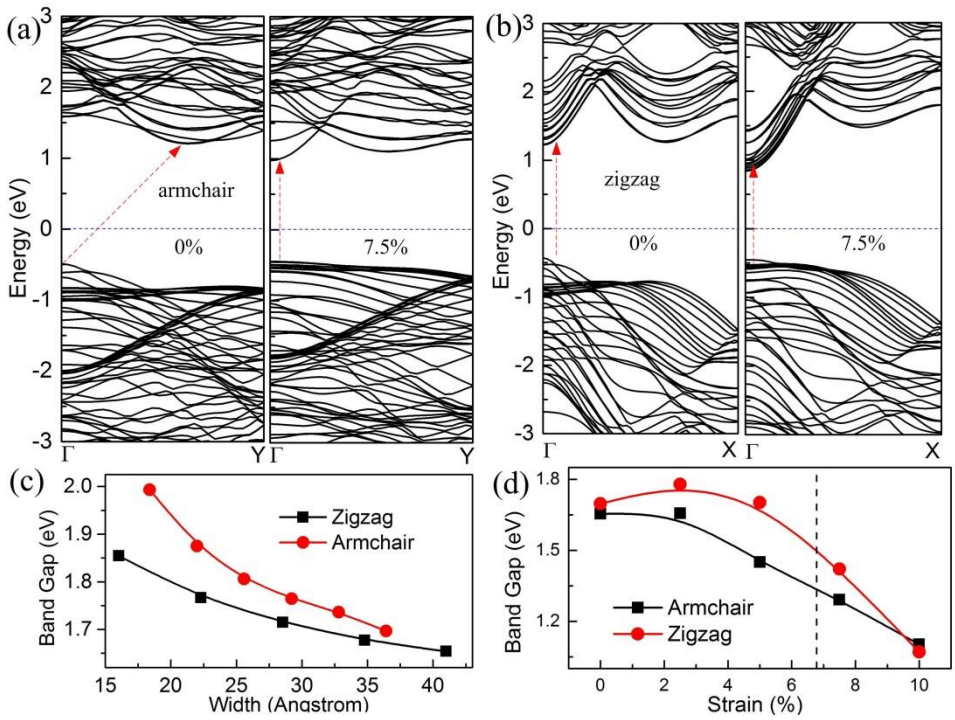

Figure 4: (color online) Bandstructures of arsenic (a) armchair with width of 3.6 nm and (b) zigzag nanoribbons with width of 4.1 nm. In each case, two bandstructures under 0% and 7.5% are shown. Band gap variation as a function of (c) ribbon width and (d) under strain.

The alloying the group-V elements themselves can produce unexpected results, such as $Bi_{1-x}Sb_x$ which can be semi metallic or semiconducting depending on the proportion x.[29,30] Recently chemical ordered alloying composed with Sb and As is also synthesized, it shares the same crystallographic structure as bulk grey arsenic (R3m, see Fig. 1 of Ref.31). We thus also studied the structural characteristics using the monolayer arsenic model, but replacing half the As in the same plane with Sb, see Fig. 1(b). From structural optimization, we can get the geometry with minimum total energy with lattice constant a_2=3.86 Å and nearest neighbour As-Sb distance d=2.7 Å, the buckling height along z direction is also larger than the value of monolayer arsenic, 1.5 Å.

The alloy AsSb exhibits the similar electronic properties as shown in Fig. 5. Monolayer AsSb is also an indirect semiconductor while the bilayer one is a semimetal with pseudogap. However, several remarkable differences can be observed. The indirect band gap (1.25 eV) of monolayer AsSb is significantly smaller than the value of arsenic while HSE calculations will not change the conclusion. The second difference is the Rashba band splitting, we can observe an obvious band flip from the band states, which might find extensive application in

spintronic devices like BiTeX (X=Cl, Br and I).[32] The phenomena is originated from strong intrinsic spin orbit coupling in antimony and asymmetric structure (arsenic and antimony are not at the same plane), see Fig. 1(b).

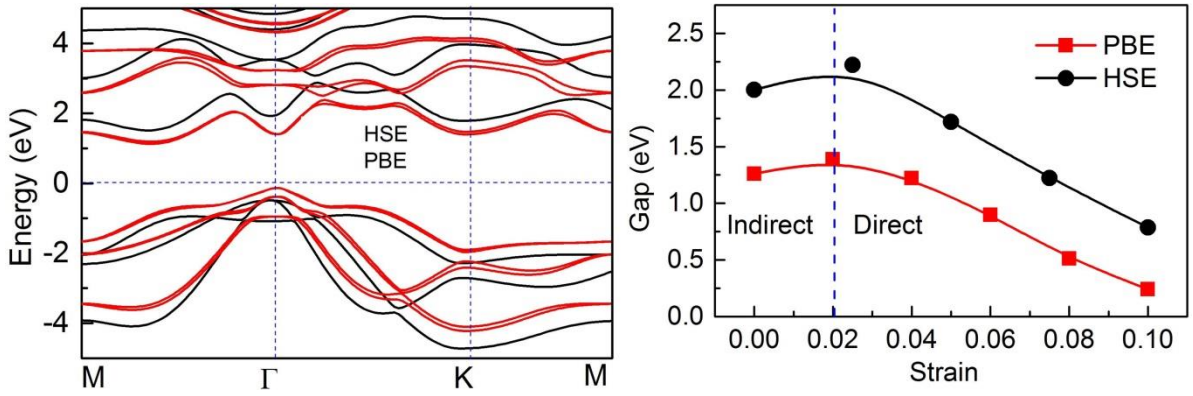

Figure 5: (color online) (a) Bandstructures of monolayer AsSb. (b) Band gap variation under strain.

In conclusion, we investigated the structural, electronic properties as well as the external strain deformation effect of two group -V layered materials, arsenic and AsSb. Both of them are found to form low-buckled two-dimensional hexagonal structures, while interlayer interaction is dominated with van der Waals interaction. Monolayer arsenic and AsSb are indirect band semiconductors, but an additional layer on top will change them to metallic. An indirect to direct band transition can be obtained when small tensile strain is applied, which would be useful for optoelectronics applications.

Acknowledgement

We would like to acknowledge the computational time provided by NCI (LE120100181 - Enhanced merit-based access and support at the new NCI petascale supercomputing facility (2012-2015)). L. K., T. F. and A. D. acknowledge the financial support (for exchange and visiting) by DAAD/PPP-ATN 57058295.

References

(1) M. Xu, T. Liang, M. Shi, H. Chen, Chem. Rev. 113, 3766 (2013).

(2) Z. Sun, H. Chang, ACS Nano 8, 4133 (2014).

(3) A. K. Geim, K. S. Novoselov, Nat. Mater. 6, 183 (2007).

(4) A. H. Castro Neto, N. M. R. Peres, K. S. Novoselov, A. K. Geim, Rev. Mod. Phys. 81, 109 (2009).

(5) P. Vogt, P. De Padova, C. Quaresima, J. Avila, E. Frantzeskakis, M. C. Asensio, A. Resta, B. Ealet, G. Le Lay, Phys. Rev. Lett. 108, 155501 (2012).

(6) A. Fleurence, R. Friedlein, T. Ozaki, H. Kawai, Y. Wang, Y. Yamada-Takamura, Phys. Rev. Lett. 108, 245501 (2012).

(7) D. Jose, A. Datta, Acc. Chem, Res. 47, 593 (2014).

(8) C. Jin, F. Lin, K. Suenaga, S. Iijima, Phys. Rev. Lett. 102, 195505 (2009).

(9) C. Lee, Q. Li, W. Kalb, X. Z. Liu, H. Berger, R. W. Carpick, J. Hone, Science, 328, 76 (2009).

(10) W. Lei, D. Portehault, D. Liu, S. Qin, Y. Chen, Nature Comm. 4, 1777 (2013).

(11) Q. H. Wang, K. Kalantar-Zadeh, A.; Kis, J. N. Coleman, M. S. Strano, Nature Nanotech. 7, 699 (2012).

(12) L. Li, Y. Yu, G. J. Ye, Q. Ge, X. Ou, H. Wu, D. Feng, X. H. Chen, Y. Zhang, Y. Nat. Nanotechnol. 9, 372 (2014).

(13) L. Kou, T. Frauenheim and C. Chen, J. Phys. Chem. Lett. 5, 2675 (2014).

(14) Z. Liu, C.-X. Liu, Y.-S. Wu, W.-H. Duan, F. Liu and J. Wu, Phys. Rev. Lett. 107, 136805 (2011).

(15) L. Kou, B.Yan, F. Hu, S.-C. Wu, T. Wehling, C. Felser, C. Chen and T. Frauenheim, Nano Lett., 13, 6251 (2013).

(16) L. Kou, S.-C. Wu, C. Felser, T. Frauenheim, C. Chen and B. Yan, ACS Nano, 8, 10448 (2014).

(17) C.-C. Liu, W. Feng and Y. Yao, Phys. Rev. Lett. 107, 076802 (2011).

(18) Y. Xu, B. Yan, H.-J. Zhang, J. Wang, G. Xu, P. Tang, W. Duan and S.-C. Zhang, Phys. Rev. Lett. 111, 136804 (2013).

(19) F.-C. Chuang, C.-H. Hsu, C.-Y. Chen, Z.-Q. Huang, V. Ozolins, H. Lin and A. Bansil, Appl. Phys. Lett. 102, 022424 (2013)

(20) C.-L. Gao, D. Qian, C.-H. Liu, J.-F. Jia and L. Feng, Chin. Phys. B 22, 067304, (2013).

(21) N. C. Norman, Chemistry of Arsenic, Antimony and Bismuth. Springer. p. 50. ISBN 978-0-7514-0389-3 (1998).

(22) G. Kresse, J. Furthm uller, Phys. Rev. B 54, 11169(1996).

(23) J. P. Perdew, K. Burke, and M. Ernzerhof. Phys. Rev. Lett., 77, 3865 (1996).

(24) J. Heyd, G. E. Scuseria, and M. Ernzerhof, J. Chem. Phys., 118, 8207 (2003).

(25) S. Grimme, J. Comput. Chem. 27, 1787 (2006).

(26) K. Refson, P. R. Tulip, S. Clark, J. Phys. Rev. B 73, 155114 (2006).
(27) J. Yoon, S. Jo, I. S. Chun, I. Jung, H.-S. Kim, M. Meitl, E. Menard, X. Li, James J. Coleman, U. Paik and J. A. Rogers, Nature 465, 329 (2010).
(28) G. R. Toniolo, J. Anversa, Cl. L. dos Santos, P. Piquini, Phy. Lett. A 378 2872 (2014).
(29) A. L. Jain, Phys. Rev. 114, 1518 (1959).
(30) A. Ibrahim and D. Thompson, Mater. Chem. Phys. 12, 29 (1985).
(31) D. P. Shoemaker, T. C. Chasapis, D. Do, M. C. Francisco, D. Y. Chung, S. D. Mahanti, A. Llobet and M. G. Kanatzidis, Phys. Rev. B 87, 094201 (2013).
(32) K. Ishizaka, et al., Nature Mater. 10, 521 (2011)